Radevici, Ivan; Sadi, Toufik; Tripurari, Tripathi; Tiira, Jonna; Ranta, Sanna; Tukiainen, Antti; Guina, Mircea; Oksanen, Jani

Observation of local electroluminescent cooling and identifying the remaining challenges

Published in:
Photonic Heat Engines

DOI:
10.1117/12.2505814

Published: 01/01/2019

Document Version
Publisher's PDF, also known as Version of record

Observation of local electroluminescent cooling and identifying the remaining challenges

Ivan Radevici, Toufik Sadi, Tripathi Tripurari, Jonna Tiira, Sanna Ranta, et al.

Ivan Radevici, Toufik Sadi, Tripathi Tripurari, Jonna Tiira, Sanna Ranta, Antti Tukiainen, Mircea Guina, Jani Oksanen, "Observation of local electroluminescent cooling and identifying the remaining challenges," Proc. SPIE 10936, Photonic Heat Engines: Science and Applications, 109360A (1 March 2019); doi: 10.1117/12.2505814

SPIE.

Event: SPIE OPTO, 2019, San Francisco, California, United States

Invited Paper

Observation of local electroluminescent cooling and identifying the remaining challenges

Ivan Radevici[a], Toufik Sadi[a], Tripathi Tripurari[a], Jonna Tiira[a], Sanna Ranta[b], Antti Tukiainen[b], Mircea Guina[b], and Jani Oksanen[a]

[a]Engineered Nanosystems Group, Aalto University, Aalto 00076, Finland
[b]The Optoelectronics Research Centre, Tampere University of Technology, P.O. Box 692, FI-33101, Finland.

ABSTRACT

The cooling of a light emitting diode (LED) by photons carrying out more energy than was used to electrically bias the device, has been predicted decades ago.[1,2] While this effect, known as electroluminescent cooling (ELC), may allow e.g. fabricating thermophotonic heat pumps (THP) providing higher efficiencies than the existing solid state coolers,[3] ELC at powers sufficient for practical applications is still not demonstrated.

To study high-power ELC we use double diode structures (DDSs), which consist of a double heterojunction (DHJ) LED and a photodiode (PD) grown within a single technological process and, thus, enclosed in a cavity with a homogeneous refractive index.[4,5] The presence of the PD in the structure allows to more directly probe the efficiency of the LED, without the need for light extraction from the system, reducing undesirable losses. Our analysis of experimentally measured $I-V$ curves for both the LED and the PD suggests that the local efficiency of the high-performance LEDs we have fabricated is approximately 110%, exceeding unity over a wide range of injection current densities of up to about $100\mathrm{A/cm}^2$.

At present the efficiency of the full DDS, however, still falls short of unity, not allowing direct evidence of the extraction of thermal energy from the LED. Here we review our previous studies of DDS for high-power EL cooling and discuss in more detail the remaining bottlenecks for demonstrating high-power ELC in the DDS context: the LED surface states, resistive and photodetection losses. In particular we report our first surface passivation measurements. Further optimization therefore mainly involves reducing the influence of the surface states, e.g. using more efficient surface passivation techniques and optimizing the PD. This combined with the optimization of the DDS layer thicknesses and contact metallization schemes is expected to finally allow purely experimental observation of high-power ELC.

Keywords: electroluminescent cooling, quantum efficiency, III-V semiconductors, surface states, double diode structures

1. INTRODUCTION

The idea of electroluminescent (EL) cooling appeared more than 60 years ago with pioneering works by Lehovec and Tauc.[1,2] However, the first experimental signs of its feasibility were reported by Dousmanis,[6] who observed in the spectrum of GaAs light emitting diode (LED) photons with an energy higher than that corresponding to the biasing voltage. The explanation for this phenomenon was the same as that for the photoluminescent (PL) cooling, anticipated in the beginning of the last century.[7] In both PL and EL processes the excess of energy carried out by photons is provided by the heat extracted from the active material. While the nature of PL and EL cooling is similar: reduction of the lattice heat by thermalization of non-equilibrium charge carriers, the dynamics of these cooling processes is completely different.

In the case of PL cooling exciting the system generally requires an incident photon with an energy larger than the band gap or the separation between the ground state and the lowest excited state. After their generation, the

Corresponding author: Ivan Radevici
E-mail: ivan.radevici@aalto.fi

Photonic Heat Engines: Science and Applications, edited by Denis V. Seletskiy, Richard I. Epstein, Mansoor Sheik-Bahae, Proc. of SPIE Vol. 10936, 109360A
 · doi: 10.1117/12.2505814

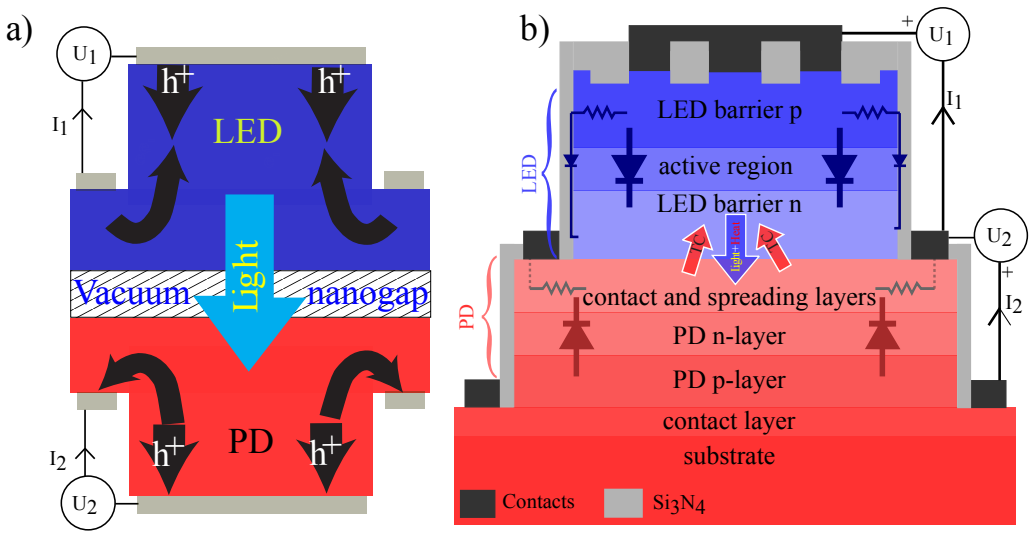

Figure 1. Schematic representation of the thermophotonic heat-pump (a), and its simplified research prototype - the double diode structure (b).

non-equilibrium charge carriers thermalize within the states manifolds, and finally recombine emitting another photon with a frequency higher than that of the incident one. The amount of thermal energy carried out by such a photon is determined by the thermal and energy distribution of the states, and, as such, is typically limited by the available thermal energy to a few kT at most.

In contrast to PL cooling, in which the absorption of heat takes place after the localized generation of non-equilibrium carriers at a recombination center, in EL cooling the electrons and holes are generated at spatially different locations, and the formation of the electron-hole pair itself is assisted by phonon absorption. In this case the electron-hole pair generation process is not limited by the absorption threshold determined by the semiconductor band gap, but by the probability that the available thermal and electrical energy can independently produce the electrons and holes. This difference has also enabled the first experimental demonstrations of ELC, at bias voltages of 60μV and power levels of $\sim$ 50pW.[8,9]

The best reported external quantum efficiencies for GaN and GaAs LED are 81%[10] and 68%,[11] respectively. However, reported internal quantum efficiencies of GaAs material are much higher exceeding 99%[12] and indicating that the efficiencies of LEDs are mainly limited due to technological difficulties in fabrication. To reduce the number of fabrication challenges especially related to light extraction, we have recently studied high-power ELC cooling using a simplified prototype of a thermophotonic heat-pump (THP), as illustrated in Figs. 1-a-b.[3]

The THP as well as the simplified double diode structure (DDS) of Fig. 1-b consist of an emitter and an absorber enclosed in the optical cavity with the same refractive index to avoid possible internal reflection. The emitter represents an LED operating in the EL cooling regime, while the absorber is a photodiode (PD) allowing to partially recycle the optical energy obtained from the emitter. To create a temperature difference between the hot (absorber) and cold (emitter) sides of the THP, as well as to avoid heat diffusion between them, the LED and PD should be thermally isolated, for example, by a vacuum nanogap. However, for the simplification of manufacturing the presently studied DDS does not use a thermal insulator.

The DDS allows to directly monitor the efficiency of the LED by the simultaneous measurement of both LED (I_1) and PD (I_2) currents. The ratio of these currents will define a figure of merit for the DDS, that we call the coupling quantum efficiency (CQE) $\eta_{CQE} = I_2/I_1$. Generally speaking, the DDS may be viewed as an LED connected to a non-ideal integrated sphere. Within this approximation the CQE estimates the lower limit of the energy transfer within the DDS structures.

In this paper, we generalize and summarize our previous results[4,5,13,14] on analyzing the performance of the DDS from the point of view of high-power EL cooling. Additionally, here we separately analyze the LED itself

Table 1. Layer structure of the DDSs based on using AlGaAs or GaInP DHJ barriers.

Layer function	DDS-AlGaAs			DDS-GaInP		
	material	doping (cm^{-3})	thickness (nm)	material	doping (cm^{-3})	thickness (nm)
contact layer	p-GaAs	1.0e19	20	p-GaAs	1.2e19	20
LED barrier p	p-$Al_{0.5}Ga_{0.5}As$	1.0e19	200	p-$Al_{0.3}Ga_{0.7}As$	1.0e19	50
				p-$Al_{0.3}Ga_{0.7}As$	3.0e17	350
	p-$Al_{0.3}Ga_{0.7}As$	3.0e17	500	p-$Ga_{0.52}In_{0.48}P$	1.0e19	50
				p-$Ga_{0.52}In_{0.48}P$	3.0e17	450
active region	i-GaAs	-	300	i-GaAs	-	800
LED barrier n and etch stop	n-$Al_{0.3}Ga_{0.7}As$	1.3e17	300	n-$Ga_{0.52}In_{0.48}P$	1.3e17	300
	n-$Al_{0.5}Ga_{0.5}As$	1.3e17	800			
	n-AlAs	1.0e18	15			
contact and spreading	n-GaAs	5.6e18	20	n-GaAs	7.5e18	20
				n-$Al_{0.3}Ga_{0.7}As$	5.0e18	800
PD n-layer	n-GaAs	1.0e18	700	n-GaAs	1.0e18	700
PD p-layer	p-GaAs	3.0e17	3000	p-GaAs	5.0e17	3000
etch stop	p-AlAs	3.0e18	15	p-AlAs	3.4e19	20
contact layer	p-GaAs	1.0e19	20	p-GaAs	1.0e19	20
buffers	p-GaAs	5.0e18	-	p-$Ga_{0.52}In_{0.48}P$	2.5e18	300
				p-GaAs	5.0e18	100
				p-$Ga_{0.52}In_{0.48}P$	2.5e18	100
				p-GaAs	5.0e18	100
substrate	p-GaAs	1.0e18	-	p-GaAs	1.0e18	-

and identify challenges for observing the of high-power EL cooling. Finally, we discuss experimental evidence that our research prototypes may already demonstrate some local EL cooling.

2. EXPERIMENTAL METHODS

This far our experiments have involved mainly DDSs with either AlGaAs or GaInP barriers in the double heterojunction (DHJ) LEDs. The best structures studied here were obtained by metal-organic chemical vapour deposition (MOCVD) and molecular beam epitaxy (MBE) for the AlGaAs and GaInP barriers, respectively. Standard UV-lithography and selective wet chemical etching procedures were applied to produce mesas with LED diameters of 100, 200, 500 and 1000 μm.[4] The detailed layer structures of the DDSs are given in Table 1.

The contacting scheme (Ni/AuGe for n-type GaAs and AuZn for p-type GaAs) was the same for all the studied samples. A measured contact resistance of $\sim 7 \cdot 10^{-5}\Omega{\cdot}cm^2$ for both n- and p-type contacts allows to neglect the contact losses in further analysis. However, different contact layouts were used to adapt the samples for various experimental characterizations. Most imporatantly, (i) for the study of the spatial distribution of the LED emission the top LED contact contained holes for direct detection of the EL emission intensity,[5] and (ii) to estimate the DDS efficiency, an omnidirectional reflector (ODR) pattern was made for the top LED contact.[15] In case of the ODR a large part of the top contact p-GaAs layer was etched away and replaced with silicon nitride providing much better reflectivity. The contact to the GaAs was made through openings in the silicon nitride layer and varied from 5 to 100 % of the top LED area.[5]

A three point scheme with a common grounded cathode for the LED and PD was used for the analysis of the electrical characteristics of the DDS. The used setup allows biasing the LED with a voltage U_1 and the simultaneous measurement of both the LED current I_1 and PD current I_2, while the PD is under a short circuit condition. The two channel source-meter used for electrical characterization allows the detection of currents higher than 10^{-9}A and a continuous injection of up to 1.5A. However, to avoid overheating of DDS all measurements with the LED injection current higher than 100 mA were performed in pulse mode with pulses <1 ms long and a 2 s delay between them. Standard tungsten probe needles were used for contacting the DDS. To measure $I-V$-$I-V$ curves of all the DDSs on the processed wafer a specialized automated setup was made to avoid human factor in the multiple measurements.

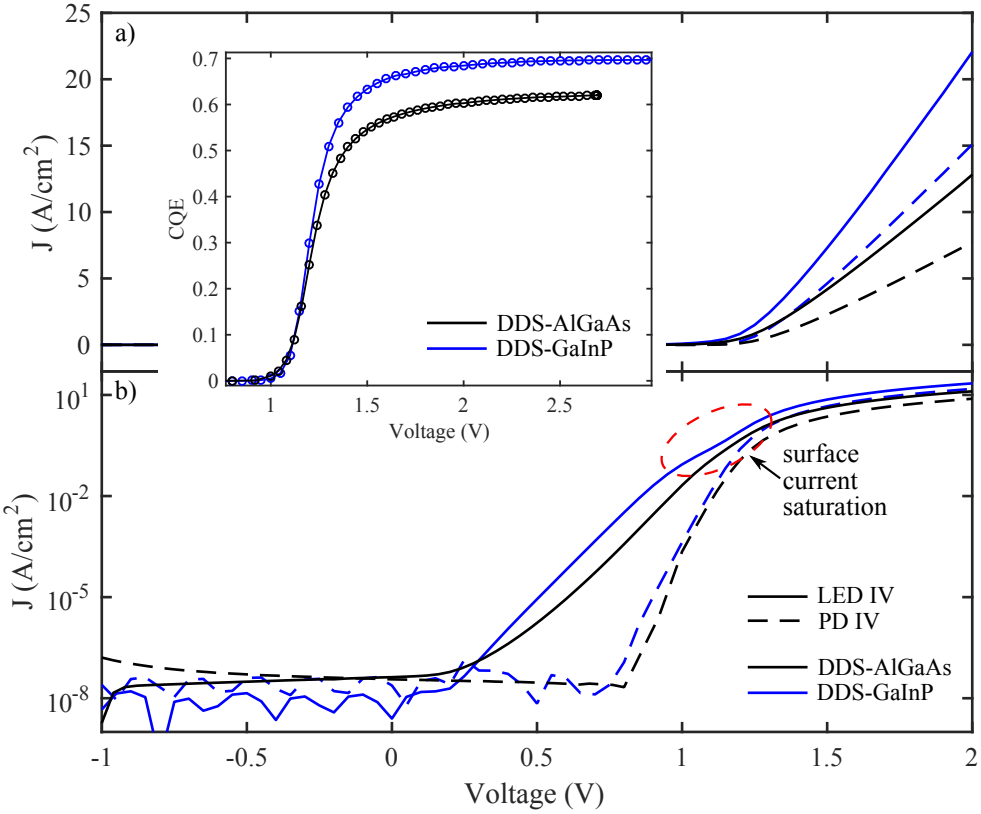

Figure 2. Electrical characteristics of the DDS structures with the highest detected efficiencies for a linear (a) and semilogarithmic (b) scales. Inset shows the dependence of the CQE on the applied LED bias for the same structures. The higher absolute currents in the GaInP DDS reflect the larger total recombination rate in the thicker active region. The black (blue) lines represent the AlGaAs (GaInP) structures, and the solid (dashed) lines the LED (PD) currents.

3. RESULTS AND DISCUSSION

3.1 Electrical characteristics

The dependence of the LED and PD currents on the LED bias for selected DDSs with AlGaAs and GaInP DHJ LEDs is presented in Fig. 2. The $I-V$ characteristics show the expected diode behaviour for both AlGaAs and GaInP DDS. However, at LED biases exceeding ~1.3-1.4 V the curves deviate from the exponential dependence due to the ohmic losses. The fit of the purely exponential part of the curve allows to estimate the ideality factors, which are equal to 1 for both LEDs and 2 for both PDs. The ideality factor of the LEDs allows to conclude that recombination in the emitter is mainly of non-radiative Shockley-Read-Hall (SRH) nature up to the voltages of $\sim 1-1.1$ V. At the same time the voltage dependence of the PD current, which follows the dependence of the LED emission on applied voltage, suggests that radiative recombination in LED is mainly bimolecular.

The LED $I-V$ curve demonstrates a clear irregularity at $\sim$ 1.1V. More detailed analysis, performed in section 3.3, suggests that this shoulder is produced by the saturation of the surface current that is an alternative way for non-radiative recombination of charge carriers.[14,15]

One of the most obvious parameters containing information about the energy transfer between the coupled diodes that can be extracted from experimentally measured $I-V$-$I-V$ curves is the ratio of PD and LED currents. We define the coupled quantum efficiency (CQE) as $\eta_{CQE} = I_2/I_1$, where I_1 is LED injected current and I_2 is the photocurrent generated in the PD under short circuit conditions. The CQE dependence on the LED bias for both the AlGaAs and GaInP structures is given in the inset to Fig. 2. The ~ 10 % difference in the maximum value of the CQE for the AlGaAs and GaInP samples most probably can be explained by the generally

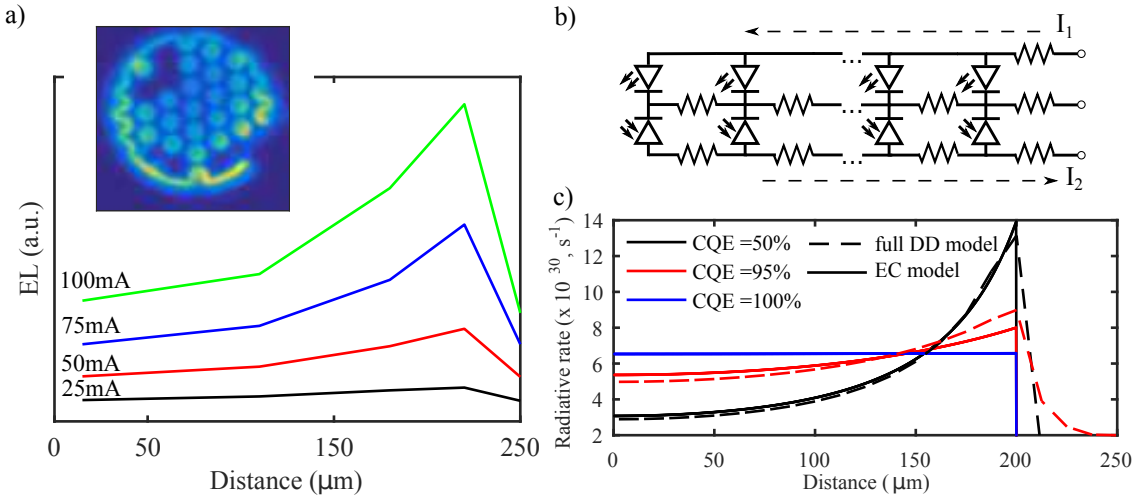

Figure 3. (a) Radial distribution of the recombination rate in the DDS LED as measured through the openings in the top contact. Inset: mapping of the LED emission at 100 mA current for 500 μm DDS size with AlGaAs barriers with holes in the metal contact to allow imaging. (b) EC model used to estimate currents in the LED and PD. (c) Comparison of the recombination rates in the LED active region at different CQEs obtained from drift-diffusion and EC models for a total LED current of 50 mA (25.4 A cm^{-2}).

higher recombination rate at the GaAs/AlGaAs interfaces as compared to GaAs/GaInP. In general the CQE provides a metric very similar to the conventional LED external quantum efficiency (EQE) also representing the lower limit of the LED internal quantum efficiency (IQE). In the DDS it additionally represents a lower limit of the energy transfer between the LED and PD. It should also be mentioned that the CQE can be represented as a product of both PD and LED efficiencies, however, the PD efficiency does not directly affect the cooling capabilities of the LED. This means that for the estimation of the real cooling efficiency of the LED we need to estimate the PD losses and subtract them from the DDS efficiency.

Generally speaking, the analysis of the DDS electrical characteristics allows to identify at least three factors reducing the efficiency of the DDS, and, thus, preventing the direct observation of EL cooling: (i) ohmic losses leading to current crowding issues, (ii) non-radiative recombination through the surface states, and (iii) detection losses in the PD. In the next sections these loss mechanisms will be analysed in more details.

3.2 Analysis of resistive losses

In the resistively limited region of the I-V curve in Fig. 2, the resistance of the setup is approximately 4 Ω. There are a few possible sources for the resistive losses in the DDS structures: (i) the external resistance in connection wires and probe needles, (ii) the contact resistance, (iii) the differential resistance in the junction itself, (iv) the resistance in the lateral current spreading layers extending beyond the LED mesa and (v) the resistance of the lateral current spreading under the LED. The external resistance in wires and probes can be easily eliminated using, for example, the 4-wire measurement technique and, as being in no way a fundamental limitation, will not be considered here. The contact resistance experimentally determined for the studied samples does not exceed $\sim 7 \cdot 10^{-5} \Omega \cdot \mathrm{cm}^2$ for both n- and p-type contacts, so it can not be considered as a notable limiting factor either. The differential resistance of the junction estimated from the ideal diode equation is still ∼40 times smaller than the resistance extracted from the experimental $I - V$ curve of the LED at high biases. This allows to conclude that the internal resistances (iv)-(v) in the DDS current spreading layer between absorber and emitter are the main sources of resistive losses. Of these, resistance (iv) can be ideally eliminated by geometric modifications in the DDS structure, while the resistance below the LED mesa itself is of more fundamental nature if a large mesa area is required. This contribution is discussed earlier[5] and below.

To study the relation between the resistive losses in the current spreading layer and the light emission a spacial mapping of the EL intensity of the LED in the DDS was performed.[5] Fig. 3-a shows the dependence of

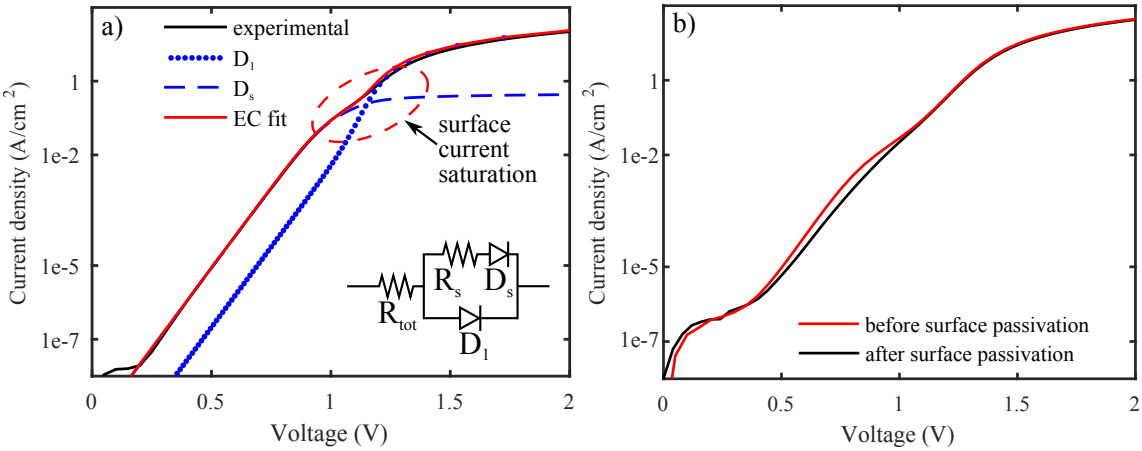

Figure 4. (a) Fitting of the experimental $I-V$ curve for DDS with GaInP barriers with EC shown in inset. (b) First experimental results showing influence of surface passivation with ammonium sulfide on $I-V$ characteristics of LED with GaInP barriers.

the EL intensity on the distance from the DDS center at a few different currents. It can be observed that EL intensity is significantly lower at the center of the DDS, especially for the high injection currents, that is typical of the current spreading difficulties even for the conventional LEDs.

One of the key differences between the conventional LED and the DDS is the presence of the PD in the latter device. The PD can significantly affect the effective conductivity of the current spreading layer, influencing the spatial EL distribution. The DDS electrical characteristics can be modelled with the equivalent circuit (EC) presented in Fig. 3-b. In general, the current in the LED terminal can be expressed as $I_1 = I_2 + I_{common} = \eta_{CQE} I_1 + I_{common}$, thus, $I_1 = I_{common(sc)}/(1-\eta_{CQE})$. This indicates that the efficiency of the DDS will substantially affect the lateral currents in the LED in general and the current spreading in particular.

More detailed numerical analysis of the current distribution in the DDS with different CQEs, performed with both EC from Fig. 3-b and full drift-diffusion (DD) model, demonstrates that the radiative recombination rate spatial profile flattens with the increase of the DDS efficiency, as shown in Fig. 3-c. Thus, the increase in the CQE reduces the pumping power needed for the operation of the DDS by the partial recycling of the current produced by the PD and improves current spreading in the device contact layers. These effects will lead to further improvement of the CQE, that will reciprocally improve the current distribution. This dependence of CQE and current distributions allows to conclude that the internal resistance in the current spreading layers is not a fundamental limiting factor for the EL cooling demonstration within the DDS approach. Even more, interaction between absorber and emitter in the DDS geometry favors improvement of the LED efficiency.[5]

3.3 Analysis of surface states

For the most part, the electrical characteristics presented in Fig. 2 demonstrate expected diode behaviour for the LEDs in the DDSs. However at ~ 1.1 V a non-ideal feature can be observed on the J-V curves of all the studied mesas. The repeating appearance of this irregularity, as well as its dependence on the LED layer structure (for the AlGaAs sample the shoulder is less pronounce), indicates that it is a device property instead of a random deviation. To understand the origin of this irregularity we modeled electrical characteristics of the LED using a simple diode equation and an equivalent circuits shown in Fig. 4-a.

The equivalent circuit assumes that LED current in the real DDS flows through the one of two possible parallel channels. The first one, presented on the top branch of the EC in Fig. 4-a, is determined by the surface states on the external mesa edge and can be analyzed as a diode with an additional resistance in series. Another current channel represents the LED diode itself and is located in the lower branch of the equivalent circuit. The Fig. 4-a shows contributions of the currents in different branches of the equivalent circuit, as well as the comparison between the nearly overlapping total modelled current and the experimentally measured current.

The modelling results suggest that at lower bias voltages the surface current on the DDS mesa walls dominate. This agrees with the extraction of the ideality factor (see subsection 3.1), suggesting that at lower biases recombination in the LED is mainly non-radiative SRH. At higher biases surface currents saturate, and influence of the diode in the LED bulk part starts to be more important. However, the surface recombination channel still contributes to the total current reducing the radiative efficiency of the device, even at working biases.

To confirm the role of the surface states we tested a standard sulfide based surface passivation technique to passivate the mesa surface.[16] Ammonium ions from the solution will remove the native oxides from the sample surfaces, and sulphur will protect the surfaces from immediate oxidation in the normal ambient conditions. Figure 4-b shows our initial results on how treating of the samples in ammonium sulfide solution affects the $I-V$ curve of LED in the GaInP DDS. Treating in ammonium sulfide solution reduces the current at low biases, where recombination on the surfaces states dominates. Also, the irregularity associated with the surface currents disappears, allowing to assume that influence of the DDS surface on its efficiency can be reduced. A very similar behaviour of the $I-V$ curves of passivated AlGaAs DDS samples was reported earlier.[17]

While the passivation reduces the current density by up to a factor of 4 at small currents, the reduction of the current is generally much smaller than expected based on comparing Figs.4-a and -b. Taking into account that the shoulder completely disappears after the passivation, it might suggest that the recombination at the interfaces between the barrier layers and active region has a substantially larger contribution than we would expect. In any case, the result presented here indicate that understanding of the recombination through parasitic channels at surfaces or interfaces still requires further tests and analysis.

3.4 Analysis of intrinsic LED efficiency

While the DDS is an attractive model for studying ELC, its performance reflects the properties of both the absorber and the emitter, i.e. $\eta_{CQE} = \eta_{LED}\eta_{PD}$. At the same time, the efficiency of the photodiode does not have a direct influence on the cooling capability of the LED itself since the absorber just facilitates the photon extraction and gives a simple way to monitor efficiency of LED. There are no simple experimental ways to directly separate efficiency of the LED from the efficiency of the PD, but being able to analyze them separately is of extreme importance for the further optimization of DDS and understanding of the origin of losses.

The current injected in the DDS satisfies $I_1 = I_{LED} + I_s$, where I_{LED} may be written in the form given by ABC-model $I_{LED} = qV_R[An + Bn^2 + Cn^3]$, where n is carrier density, q is the elementary charge, V_R is recombination volume, and A, B and C are the SRH, bimolecular (radiative) and Auger recombination parameters of the diode, respectively, and I_s is the surface current that can be extracted from using the equivalent circuit described in section 3.3. The general form of the photocurrent I_{PD} generated in the absorber may correspondingly be expressed as

$$I_{PD} = qV_R\eta_{PD}Bn^2, \tag{1}$$

where η_{PD} is the photodetection efficiency which by definition describes the ratio between the photocurrent in the PD and the total radiative recombination in the LED. This factor therefore accounts for all the optical losses in the DDS as well as all the non-idealities of the PD. Defining an auxiliary coupling function as $F = (I_{LED} - I_s)/\sqrt{I_{PD}}$ and substituting I_{LED} and n, computed from I_{PD} into it we obtain

$$F = \frac{I_1 - I_s}{\sqrt{I_{PD}}} = A\sqrt{\frac{qV_r}{\eta_{PD}B}} + \frac{\sqrt{I_{PD}}}{\eta_{PD}} + \frac{C}{\sqrt{qV_r}}\left(\frac{1}{\eta_{PD}B}\right)^{3/2} I_{PD}. \tag{2}$$

From this representation it is evident that the photodetection efficiency η_{PD} can be estimated by fitting a second order polynomial to the auxiliary coupling function F plotted as a function of $\sqrt{I_{PD}}$. For the samples, whose $I-V$ curves are presented in Fig.2 the η_{PD} is 66 % and 71 % for samples with AlGaAs and GaInP barriers, respectively.

In general, a high CQE alone is not sufficient for demonstration of EL cooling. The LED bias must also be low enough for the power conversion efficiency (PCE) to satisfy the condition $\eta_{PCE} = \eta_{CQE} \times (\hbar\omega/qU) > 1$, where U is the real bias voltage over the LED not including the additional external resistive losses arising e.g. from the measurement setup, which dominates the LED resistance in our case, and $\hbar\omega$ =1.42 eV is a photon

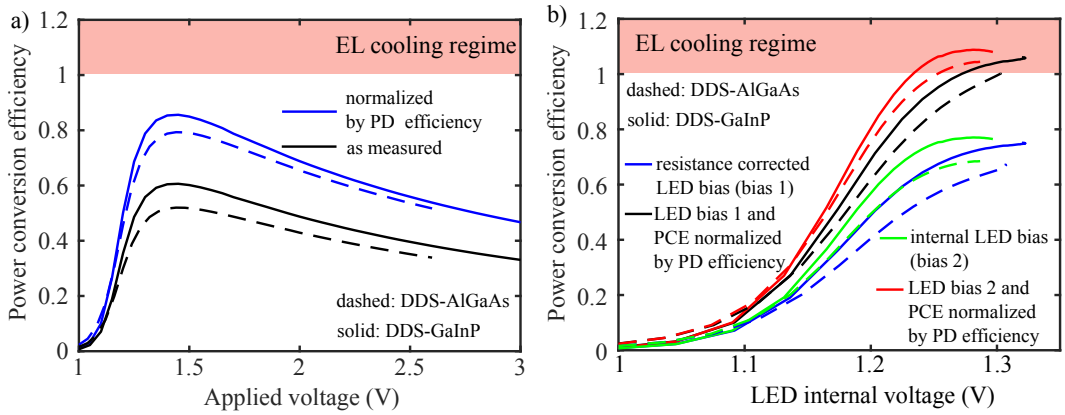

Figure 5. (a) Lower bound for the power conversion efficiency of the LED as directly evaluated using the measured CQE and normalized by the photodetection efficiency, as a function of bias applied over the LED. The dashed lines show results for DDS with AlGaAs barriers, the solid lines are for the GaInP DDS. (b) The PCE curves as a function of the LED bias estimated by elimination of the resistive losses in the measurement setup (bias 1) and by using the PD photocurrent (bias 2) to estimate the internal LED voltage. At values above unity EL cooling takes place.

energy corresponding to the room temperature GaAs bandgap, which slightly underestimates the average photon energy. Fig. 5-a compares the PCE for the DDS with AlGaAs and GaInP barriers as measured and normalized by η_{PD} when the LED bias is considered to directly correspond to the applied bias. While the efficiency of DDS is significantly higher for both samples it is still insufficient for reaching EL cooling regime.

However, as it was discussed in section 3.2, resistive losses in DDS can be potentially mostly eliminated, and thus can not be considered as a fundamental limitation. The Fig. 5-b shows the dependence of the PCE of the studied DDS on the LED internal bias. Curve sets marked "bias 1" correspond either to the directly measured CQE or the CQE corrected by the photodetection efficiency as above, but with the external bias voltage U_1 replaced by the resistance corrected internal LED bias $U \approx U_1 - RI_1$ instead. In this case the voltage corresponds to the actual bias of the LED and does not include the ohmic losses associated with the measurement setup and the n-type current spreading layers outside the LED mesa. The series resistance R is well approximated by the differential resistance of the LED at large currents. Alternatively, and due to the uncertainties in the resistance, we also use the PD current to estimate the internal LED bias U_{LED}, since the PD current is expected to scale as $I_2 = I_{ref} \exp[q(U_{LED} - U_{ref})/kT]$, as long as the carrier densities in the LED remain sufficiently non-degenerate. These curves are marked in Fig.5-b as "bias 2". In our case, we expect that this is the case throughout the measurement regime as the predicted bias voltages remain well below the E_g/q limit.[14]

The Fig. 5-b clearly suggests that our LEDs already have high enough efficiency to operate in the EL cooling regime, and even exceed the efficiency requirement for the heat neutrality by ∼10 %. Simple analysis of heat transfer in DDS predicts that this will be enough to observe cooling of top part of the DDS by 30 mK, even considering absense of the heat isolation between absorber and emitter.

4. CONCLUSIONS

Our estimations suggest that the bulk efficiency of the high-efficiency LEDs in the DDS with either AlGaAs or GaInP barriers already exceeds the minimum requirement for localized high power EL cooling. Direct observation of exceeding the cooling barrier or cooling itself, however, will still require improving several aspects of the structures, in particular (i) reducing the resistive losses, (ii) reducing the surface recombination in the LED surface states and (iii) improving the photodetection efficiency.

Acknowledgments

This project has received funding from the Academy of Finland and the European Research Council (ERC) under the European Union's Horizon 2020 research and innovation programme (grant agreement No 638173).

We acknowledge the provision of facilities and technical support from Micronova Nanofabrication Centre at Aalto University.

REFERENCES

[1] Lehovec, K., Accardo, C. A., and Jamgochian, E., "Light emission produced by current injected into a green silicon-carbide crystal," *Phys. Rev.* **89**, 20–25 (Jan 1953).

[2] Tauc, J., "The share of thermal energy taken from the surroundings in the electro-luminescent energy radiated from a p-n junction," *Czechoslovak Journal of Physics* **7**, 275–276 (May 1957).

[3] Oksanen, J. and Tulkki, J., "Thermophotonic heat pumpa theoretical model and numerical simulations," *Journal of Applied Physics* **107**(9), 093106 (7 p.) (2010).

[4] Olsson, A., Tiira, J., Partanen, M., Hakkarainen, T., Koivusalo, E., Tukiainen, A., Guina, M., and Oksanen, J., "Optical Energy Transfer and Loss Mechanisms in Coupled Intracavity Light Emitters," *IEEE Transactions on Electron Devices* **63**, 3567–3573 (Sept. 2016).

[5] Radevici, I., Tiira, J., Sadi, T., and Oksanen, J., "Influence of photo-generated carriers on current spreading in double diode structures for electroluminescent cooling," *Semiconductor Science and Technology* , 05LT01 (Mar. 2018).

[6] Dousmanis, G. C., Mueller, C. W., Nelson, H., and Petzinger, K. G., "Evidence of Refrigerating Action by Means of Photon Emission in Semiconductor Diodes," *Physical Review* **133**, A316–A318 (Jan. 1964).

[7] Pringsheim, P., "Zwei Bemerkungen über den Unterschied von Lumineszenz- und Temperaturstrahlung," *Zeitschrift für Physik* **57**, 739–746 (Nov. 1929).

[8] Santhanam, P., Gray, D. J., and Ram, R. J., "Thermoelectrically Pumped Light-Emitting Diodes Operating above Unity Efficiency," *Physical Review Letters* **108**, 097403 (Feb. 2012).

[9] Santhanam, P., Huang, D., Ram, R. J., Remennyi, M. A., and Matveev, B. A., "Room temperature thermoelectric pumping in mid-infrared light-emitting diodes," *Applied Physics Letters* **103**, 183513 (Oct. 2013).

[10] Hurni, C. A., David, A., Cich, M. J., Aldaz, R. I., Ellis, B., Huang, K., Tyagi, A., DeLille, R. A., Craven, M. D., Steranka, F. M., et al., "Bulk GaN flip-chip violet light-emitting diodes with optimized efficiency for high-power operation," *Applied Physics Letters* **106**, 031101 (Jan. 2015).

[11] Broell, M., Sundgren, P., Rudolph, A., Schmid, W., Vogl, A., and Behringer, M., "New developments on high-efficiency infrared and InGaAlP light-emitting diodes at OSRAM Opto Semiconductors," *Proceedings of SPIE, Volume 9003, Light-Emitting Diodes: Materials, Devices, and Applications for Solid State Lighting XVIII* , 90030L (Feb. 2014).

[12] Gauck, H., Gfroerer, T. H., Renn, M. J., Cornell, E. A., and Bertness, K. A., "External radiative quantum efficiency of 96% from a GaAs / GaInP heterostructure," *Applied Physics A: Materials Science & Processing* **64**, 143–147 (Jan. 1997).

[13] Tiira, J., Radevici, I., Haggren, T., Hakkarainen, T., Kivisaari, P., Lyytikäinen, J., Aho, A., Tukiainen, A., Guina, M., and Oksanen, J., "Intracavity double diode structures with GaInP barrier layers for thermophotonic cooling," 1012109 (Feb. 2017).

[14] Radevici, I., Tiira, J., Sadi, T., Ranta, S., Tukiainen, A., Guina, M., and Oksanen, J., "Thermophotonic cooling in GaAs based light emitters," *Applied Physics Letters* , accepted for publication (2019).

[15] Sadi, T., Radevici, I., Kivisaari, P., and Oksanen, J., "Electroluminescent cooling in III-V intracavity diodes: Practical requirements," *IEEE Transactions on Electron Devices* **66** (2019). Accepted, doi: 10.1109/TED.2018.2885267.

[16] Baca, A. and Ashby, C., [*Fabrication of GaAs Devices*], IET, The Institution of Engineering and Technology, Michael Faraday House, Six Hills Way, Stevenage SG1 2AY, UK (Jan. 2005).

[17] Radevici, I., Tiira, J., and Oksanen, J., "Lock-in thermography approach for imaging the efficiency of light emitters and optical coolers," 101210Q (Feb. 2017).